Springer

Journal of
Mechanical
Science and
Technology

Journal of Mechanical Science and Technology 23 (2009) 389~400

www.springerlink.com/content/1738-494x
DOI 10.1007/s12206-008-1226-7

Development of dynamic response analysis algorithm for beam structures using transfer of mass coefficient †

M. S. Choi[1,*], D. J. Yeo[2], J. H. Byun[2], J. J. Suh[2] and J. K. Yang[2]

[1]*Department of Maritime Police Science, Chonnam National University, Yeosu, 550-749, Korea*
[2]*Faculty of Marine Technology, Chonnam National University, Yeosu, 550-749, Korea*

(Manuscript Received October 21, 2008; Revised December 6, 2008; Accepted December 29, 2008)

Abstract

The authors developed the transfer mass coefficient method (TMCM) in order to compute effectively the dynamic response of a beam structure. In this paper, the algorithm for the dynamic response analysis of a three-dimensional beam structure is formulated. Through the computation results of numerical models, which are plane and space beam structures, obtained by the transfer mass coefficient method and the direct integration method, we verify that the transfer mass coefficient method can remarkably decrease the computation time of the direct integration method without the loss of accuracy in spite of using small computer storage.

Keywords: Beam structure; Direct integration method; Dynamic response analysis; Finite element analysis; Newmark's β method; Transfer mass coefficient method

1. Introduction

The number of large and complex structures has increased rapidly with the progress of industry. It is very important to obtain an accurate dynamic response of the structures subjected to various loads in design process for the safety of the structures.

The dynamic analysis of complex structures has experienced impressive progress since the 1970s [1]. A variety of methods for obtaining the dynamic response have been developed. Among them, the two most popular methods using finite element analysis with the growth of digital computer are the mode superposition method (MSM) and the direct integration method (DIM) [1-3]. The MSM is very effective for obtaining the dynamic response of the structures by using only a few of the lowest vibration modes. However, the MSM is not valid for structures with nonlinearity and damping that is not orthogonal [1]. On the other hand, DIM, which combines the finite element analysis and the numerical integration techniques, such as Newmark's β and Wilson's θ method, can evaluate the dynamic response of structures with nonlinearities and a variety of damping types.

Both the MSM and the DIM need large computer memory and long computation time in case of requiring an accurate dynamic response of large and complex structures, because the large and complex structure is modeled as a numerical model with a large number of degrees-of-freedom. In particular, the DIM is generally very inferior to the MSM in view of computation time. Therefore, it is difficult to obtain the accurate dynamic response of large and complex structures by both methods on a personal computer. To overcome above-mentioned disadvantages, a variety of methods for the efficient dynamic response analysis are proposed by many researchers [4-10].

The step-by-step transfer matrix method [4, 5], which combines the standard transfer matrix method [11] and the numerical integration techniques, has the

† This paper was recommended for publication in revised form by Associate Editor Hong Hee Yoo

*Corresponding author. Tel.: +61 659 3183, Fax.: +82 61 659 3189
E-mail address: engine@chonnam.ac.kr

drawback that numerical instabilities often occur when time step is small and there is rigid elastic support at the intermediate part of the structure [5, 10]. The finite element-transfer matrix method [6, 7] for the dynamic response analysis has the same drawback occurring in the step-by-step transfer matrix method, too.

Inoue et al. [10] suggested a method which is derived from a combination of the transfer influence coefficient method [12, 13] and the numerical integration techniques in order to improve the accuracy and computational efficiency of the dynamic response analysis for the large structures. However, this method has many limitations for analyzing the dynamic response of structures. Because it requires that the mass matrix always exist as a diagonal matrix, a beam structure is restricted within a lumped mass system. Therefore, we cannot use a consistent mass system for a beam structure in this method, and it is difficult to adapt the algorithm for the plate, shell and solid structures later. Because this method requires that the damping matrix always be a diagonal matrix, the damping of a structure is restricted within several viscous dampers that support the structure from the base. Therefore, it is very difficult to use structural damping and Rayleigh-type damping in this method.

The purpose of this paper is to present a new method for computing effectively the dynamic response analysis of various beam structures modeled as lumped mass, consistent mass, viscous damper, structural damping and Rayleigh-type damping. We call it the transfer mass coefficient method (TMCM). In this paper, the algorithm for the dynamic response analysis of a three-dimensional beam structure is formulated by the TMCM. Plane and space beam structures are chosen as numerical models. The response results and computation times obtained by the TMCM are compared with those obtained by the DIM under the same condition.

2. Formulation

2.1 Modeling

To describe the concept of the transfer mass coefficient method, a three-dimensional beam structure is introduced as an analytical model, as shown in Fig.1.

The three-dimensional beam structure consists of beam elements, springs, dampers and crooked parts. Connecting points of adjacent beam elements and both ends of the analytical model are called as nodes. Because the excitation and response points should be included in nodes, too, we should properly separate the beam structure. For the analytical model with n beam elements, each node is called successively as node 1, node 2, …, node n+1 from the left- to right-hand ends of the model. Each node has 6 degrees-of-freedom.

A displacement vector ($\mathbf{d} = \{u_x, u_y, u_z, \phi_x, \phi_y, \phi_z\}^T$) at each node is composed of displacements (u_x, u_y, u_z) in the direction of the coordinate axes and the angular displacements (ϕ_x, ϕ_y, ϕ_z) around the coordinate axes. A velocity vector ($\mathbf{v} = d\mathbf{d}/dt = \{v_x, v_y, v_z, \omega_x, \omega_y, \omega_z\}^T$) at each node consists of linear velocities (v_x, v_y, v_z) and the angular velocities ($\omega_x, \omega_y, \omega_z$). An acceleration vector ($\mathbf{a} = d\mathbf{v}/dt = \{a_x, a_y, a_z, \alpha_x, \alpha_y, \alpha_z\}^T$) at each node is composed of linear accelerations (a_x, a_y, a_z) and the angular accelerations ($\alpha_x, \alpha_y, \alpha_z$). A force vector ($\mathbf{f} = \{F_x, F_y, F_z, M_x, M_y, M_z\}^T$) at each node consists of the forces (F_x, F_y, F_z) and the moments (M_x, M_y, M_z).

If there are some intermediate supporting parts which support the beam structure from the base, they are modeled as six springs and six viscous dampers. The springs are three linear and three rotational springs whose constants are ($\hat{k}_x, \hat{k}_y, \hat{k}_z$) and ($\hat{K}_x, \hat{K}_y, \hat{K}_z$). The viscous dampers are three linear and three rotational viscous dampers whose constants are ($\hat{c}_x, \hat{c}_y, \hat{c}_z$) and ($\hat{C}_x, \hat{C}_y, \hat{C}_z$).

In the present method, the boundary conditions of the beam structure are modeled as springs and viscous dampers supporting the first and the last nodes from the base. For example, we consider the values of the spring constants of node 1 as infinities in case of fixed condition at the left-hand end. For the free condition at the right-hand end, the values of the spring constants of node n+1 are considered as zeros.

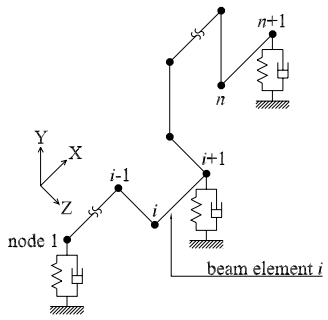

Fig. 1. Analytical model.

2.2 Transfer rule

To describe easily the concept of the present method, a node is divided into the left- and right-hand sides of the node. We denote quantities of the left-hand side of the node as with the head mark "–" on the symbols corresponding to the quantities, and quantities of the right-hand side of the node as without the head mark. Symbols with subscript *i* represent quantities corresponding to the *i*-th node or the *i*-th beam element. Symbols with superscript *i* mean quantities representing by the local coordinate system fixed on the *i*-th beam element. For example, the vector $\mathbf{f}_{i+1}^{i}$ means the force vector represented by the local coordinate system of the *i*-th beam element at the right-hand side of the (*i*+1)-th node. The vector $\bar{\mathbf{a}}_{i+1}^{i}$ means the acceleration vector represented by the local coordinate system of the *i*-th beam element at the left-hand side of the (*i*+1)-th node.

We define the relationship between the force vector ($\mathbf{f}_{i}^{i}$) and the acceleration vector ($\mathbf{a}_{i}^{i}$) as follows:

$$\mathbf{f}_{i}^{i}(t) = \mathbf{J}_{i}^{i}\mathbf{a}_{i}^{i}(t) + \mathbf{b}_{i}^{i}(t), \tag{1}$$

and the matrix $\mathbf{J}_{i}^{i}$ and the vector $\mathbf{b}_{i}^{i}$ are the mass coefficient matrix and the force corrective vector represented by the local coordinate system of the *i*-th beam element at the right-hand side of the *i*-th node.

In the same manner, the relationships between the force vectors ($\bar{\mathbf{f}}_{i+1}^{i}$, $\mathbf{f}_{i+1}^{i}$, $\mathbf{f}_{i+1}^{i+1}$) and the acceleration vectors ($\bar{\mathbf{a}}_{i+1}^{i}$, $\mathbf{a}_{i+1}^{i}$, $\mathbf{a}_{i+1}^{i+1}$) are defined as follows:

$$\bar{\mathbf{f}}_{i+1}^{i}(t) = \bar{\mathbf{J}}_{i+1}^{i}\bar{\mathbf{a}}_{i+1}^{i}(t) + \bar{\mathbf{b}}_{i+1}^{i}(t), \tag{2}$$

$$\mathbf{f}_{i+1}^{i}(t) = \mathbf{J}_{i+1}^{i}\mathbf{a}_{i+1}^{i}(t) + \mathbf{b}_{i+1}^{i}(t), \tag{3}$$

$$\mathbf{f}_{i+1}^{i+1}(t) = \mathbf{J}_{i+1}^{i+1}\mathbf{a}_{i+1}^{i+1}(t) + \mathbf{b}_{i+1}^{i+1}(t). \tag{4}$$

From the continuous condition of the displacement vectors at each node, we obtain

$$\begin{aligned} \bar{\mathbf{d}}_{i+1}^{i}(t) &= \mathbf{d}_{i+1}^{i}(t), \\ \bar{\mathbf{v}}_{i+1}^{i}(t) &= \mathbf{v}_{i+1}^{i}(t), \\ \bar{\mathbf{a}}_{i+1}^{i}(t) &= \mathbf{a}_{i+1}^{i}(t). \end{aligned} \tag{5}$$

From Newmark's β method [14], the displacement and velocity vectors at time *t* are assumed by using the displacement, velocity and acceleration vectors before time step, Δt , and the acceleration vector at the time *t*. Therefore, the displacement and velocity vectors of the *i*-th and (*i*+1)-th nodes are as follows:

$$\begin{aligned} \mathbf{d}_{i}^{i}(t) &= \beta(\Delta t)^2\,\mathbf{a}_{i}^{i}(t) + \mathbf{g}_{i}^{i}(t), \\ \mathbf{v}_{i}^{i}(t) &= \gamma\Delta t\,\mathbf{a}_{i}^{i}(t) + \mathbf{h}_{i}^{i}(t), \end{aligned} \tag{6}$$

$$\begin{aligned} \mathbf{d}_{i+1}^{i}(t) &= \beta(\Delta t)^2\,\mathbf{a}_{i+1}^{i}(t) + \mathbf{g}_{i+1}^{i}(t), \\ \mathbf{v}_{i+1}^{i}(t) &= \gamma\Delta t\,\mathbf{a}_{i+1}^{i}(t) + \mathbf{h}_{i+1}^{i}(t), \end{aligned} \tag{7}$$

where

$$\begin{aligned} \mathbf{g}_{i}^{i}(t) &= \mathbf{d}_{i}^{i}(t-\Delta t) + \Delta t\,\mathbf{v}_{i}^{i}(t-\Delta t) + \\ &\quad (0.5-\beta)(\Delta t)^2\,\mathbf{a}_{i}^{i}(t-\Delta t), \\ \mathbf{h}_{i}^{i}(t) &= \mathbf{v}_{i}^{i}(t-\Delta t) + (1-\gamma)\Delta t\,\mathbf{a}_{i}^{i}(t-\Delta t), \\ \mathbf{g}_{i+1}^{i}(t) &= \mathbf{d}_{i+1}^{i}(t-\Delta t) + \Delta t\,\mathbf{v}_{i+1}^{i}(t-\Delta t) + \\ &\quad (0.5-\beta)(\Delta t)^2\,\mathbf{a}_{i+1}^{i}(t-\Delta t), \\ \mathbf{h}_{i+1}^{i}(t) &= \mathbf{v}_{i+1}^{i}(t-\Delta t) + (1-\gamma)\Delta t\,\mathbf{a}_{i+1}^{i}(t-\Delta t), \end{aligned} \tag{8}$$

in which the parameters β and γ are chosen by considering integration accuracy and stability.

The equation of motion for the *i*-th beam element at time *t,* which is represented by the local coordinate system fixed on the *i*-th beam element, is represented as

$$\mathbf{M}_{i}^{i}\begin{Bmatrix}\mathbf{a}_{i}^{L}(t)\\ \mathbf{a}_{i}^{R}(t)\end{Bmatrix} + \mathbf{C}_{i}^{i}\begin{Bmatrix}\mathbf{v}_{i}^{L}(t)\\ \mathbf{v}_{i}^{R}(t)\end{Bmatrix} + \mathbf{K}_{i}^{i}\begin{Bmatrix}\mathbf{d}_{i}^{L}(t)\\ \mathbf{d}_{i}^{R}(t)\end{Bmatrix} = \begin{Bmatrix}\mathbf{f}_{i}^{L}(t)\\ \mathbf{f}_{i}^{R}(t)\end{Bmatrix}, \tag{9}$$

where the matrices $\mathbf{M}_{i}^{i}$, $\mathbf{C}_{i}^{i}$ and $\mathbf{K}_{i}^{i}$ are the mass, damping and stiffness matrices of the *i*-th beam element represented by the local coordinate system of the *i*-th beam element. We can use both the lumped mass system and the consistent mass system for the beam element in the present method. For the consistent mass system, the mass matrix $\mathbf{M}_{i}^{i}$ is given in appendix. In the present method, we can use structural damping and Rayleigh-type damping for the beam element. For the Rayleigh-type damping, the matrix $\mathbf{C}_{i}^{i}$ is given in the appendix. The matrix $\mathbf{K}_{i}^{i}$ given in the appendix is the general stiffness

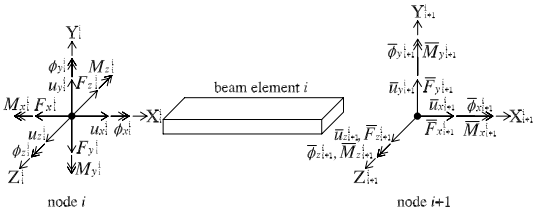

Fig. 2. Definition of positive direction of displacements and forces of the *i*-th beam element.

matrix for the beam element. The superscripts "L" and "R" of $\mathbf{a}_i(t)$, $\mathbf{v}_i(t)$, $\mathbf{d}_i(t)$ and $\mathbf{f}_i(t)$ mean the quantities of the left- and right-hand sides of the *i*-th beam element.

Because the left-hand side of the *i*-th beam element becomes the right-hand side of the *i*-th node, and the right-hand side of the *i*-th beam element becomes the left-hand side of the (*i*+1)-th node, we obtain

$$\begin{aligned}
&\mathbf{a}_i^i(t) = \mathbf{a}_i^L(t), \quad \mathbf{v}_i^i(t) = \mathbf{v}_i^L(t), \quad \mathbf{d}_i^i(t) = \mathbf{d}_i^L(t), \\
&\bar{\mathbf{a}}_{i+1}^i(t) = \mathbf{a}_i^R(t), \quad \bar{\mathbf{v}}_{i+1}^i(t) = \mathbf{v}_i^R(t), \quad \bar{\mathbf{d}}_{i+1}^i(t) = \mathbf{d}_i^R(t), \\
&\mathbf{f}_i^i(t) = -\mathbf{f}_i^L(t), \quad \bar{\mathbf{f}}_{i+1}^i(t) = \mathbf{f}_i^R(t).
\end{aligned} \tag{10}$$

Fig. 2 shows the positive directions of displacements and forces at the left- and right-hand sides of the *i*-th beam element from the viewpoint of nodes. Therefore, Eq. (9) can be changed as follows:

$$\mathbf{M}_i^i \begin{Bmatrix} \mathbf{a}_i^i(t) \\ \bar{\mathbf{a}}_{i+1}^i(t) \end{Bmatrix} + \mathbf{C}_i^i \begin{Bmatrix} \mathbf{v}_i^i(t) \\ \bar{\mathbf{v}}_{i+1}^i(t) \end{Bmatrix} + \mathbf{K}_i^i \begin{Bmatrix} \mathbf{d}_i^i(t) \\ \bar{\mathbf{d}}_{i+1}^i(t) \end{Bmatrix} = \begin{Bmatrix} -\mathbf{f}_i^i(t) \\ \bar{\mathbf{f}}_{i+1}^i(t) \end{Bmatrix}. \tag{11}$$

From substituting Eqs. (5)-(7) into Eq. (11), the following equation is obtained.

$$\begin{bmatrix} \mathbf{P}_i^i & \mathbf{Q}_i^i \\ \mathbf{R}_i^i & \mathbf{S}_i^i \end{bmatrix} \begin{Bmatrix} \mathbf{a}_i^i(t) \\ \bar{\mathbf{a}}_{i+1}^i(t) \end{Bmatrix} + \begin{Bmatrix} \mathbf{y}_i^i(t) \\ \mathbf{y}_{i+1}^i(t) \end{Bmatrix} = \begin{Bmatrix} -\mathbf{f}_i^i(t) \\ \bar{\mathbf{f}}_{i+1}^i(t) \end{Bmatrix}, \tag{12}$$

where

$$\begin{aligned}
&\begin{bmatrix} \mathbf{P}_i^i & \mathbf{Q}_i^i \\ \mathbf{R}_i^i & \mathbf{S}_i^i \end{bmatrix} = \mathbf{M}_i^i + \gamma \Delta t \mathbf{C}_i^i + \beta (\Delta t)^2 \mathbf{K}_i^i, \\
&\begin{Bmatrix} \mathbf{y}_i^i(t) \\ \mathbf{y}_{i+1}^i(t) \end{Bmatrix} = \mathbf{C}_i^i \begin{Bmatrix} \mathbf{h}_i^i(t) \\ \mathbf{h}_{i+1}^i(t) \end{Bmatrix} + \mathbf{K}_i^i \begin{Bmatrix} \mathbf{g}_i^i(t) \\ \mathbf{g}_{i+1}^i(t) \end{Bmatrix}.
\end{aligned} \tag{13}$$

Consider the transfer of the mass coefficient matrix and the force corrective vector, across the *i*-th beam element, from the right-hand side of the *i*-th node to the left-hand side of the (*i*+1)-th node. From Eqs. (1), (2) and (12), we can obtain

$$\bar{\mathbf{J}}_{i+1}^i = \mathbf{R}_i^i \mathbf{B}_i^i + \mathbf{S}_i^i, \tag{14}$$

$$\bar{\mathbf{b}}_{i+1}^i(t) = \mathbf{R}_i^i \mathbf{w}_i^i(t) + \mathbf{y}_{i+1}^i(t), \tag{15}$$

where

$$\begin{aligned}
&\mathbf{B}_i^i = \mathbf{A}_i^i \mathbf{Q}_i^i, \quad \mathbf{A}_i^i = -(\mathbf{P}_i^i + \mathbf{J}_i^i)^{-1}, \\
&\mathbf{w}_i^i(t) = \mathbf{A}_i^i \{\mathbf{b}_i^i(t) + \mathbf{y}_i^i(t)\},
\end{aligned} \tag{16}$$

and Eqs. (14) and (15) are the field transfer rules of the mass coefficient matrix and the force corrective vector, respectively.

If there are an additional mass, springs, viscous dampers and external forces at the (*i*+1)-th node, the balancing of the forces and the moments at the (*i*+1)-th node yields

$$\begin{aligned}
\hat{\mathbf{M}}_{i+1}^i \mathbf{a}_{i+1}^i(t) = \mathbf{f}_{i+1}^i(t) - \bar{\mathbf{f}}_{i+1}^i(t) - \hat{\mathbf{C}}_{i+1}^i \mathbf{v}_{i+1}^i(t) - \\
\hat{\mathbf{K}}_{i+1}^i \mathbf{d}_{i+1}^i(t) + \hat{\mathbf{q}}_{i+1}^i(t),
\end{aligned} \tag{17}$$

where

$$\begin{aligned}
&\hat{\mathbf{M}}_{i+1}^i = \mathrm{Diag}[\hat{m}, \hat{m}, \hat{m}, \hat{M}_x, \hat{M}_y, \hat{M}_z]_{i+1}^i, \\
&\hat{\mathbf{C}}_{i+1}^i = \mathrm{Diag}[\hat{c}_x, \hat{c}_y, \hat{c}_z, \hat{C}_x, \hat{C}_y, \hat{C}_z]_{i+1}^i, \\
&\hat{\mathbf{K}}_{i+1}^i = \mathrm{Diag}[\hat{k}_x, \hat{k}_y, \hat{k}_z, \hat{K}_x, \hat{K}_y, \hat{K}_z]_{i+1}^i, \\
&\hat{\mathbf{q}}_{i+1}^i = \{\hat{q}_x, \hat{q}_y, \hat{q}_z, \hat{Q}_x, \hat{Q}_y, \hat{Q}_z\}_{i+1}^{i\ T},
\end{aligned} \tag{18}$$

in which Diag[⋯] represents a diagonal matrix, the matrix $\hat{\mathbf{M}}_{i+1}^i$ consists of the additional mass ($\hat{m}$) and the rotational inertia ($\hat{M}$) at the (*i*+1)-th node. The matrices $\hat{\mathbf{K}}_{i+1}^i$ and $\hat{\mathbf{C}}_{i+1}^i$ are the stiffness and damping matrices composed of the linear and rotational springs and viscous dampers supporting the (*i*+1)-th node of the analytical model from the base. The vector $\hat{\mathbf{q}}_{i+1}^i$ is the external force vector composed of the external force ($\hat{q}$) and moment ($\hat{Q}$) acting on the (*i*+1)-th node.

Consider the transfer of the mass coefficient matrix and the force corrective vector from the left-hand side to the right-hand side of the (*i*+1)-th node. From Eqs. (2), (3), (7) and (17), we can derive

$$\mathbf{J}_{i+1}^i = \bar{\mathbf{J}}_{i+1}^i + \hat{\mathbf{M}}_{i+1}^i + \gamma \Delta t \hat{\mathbf{C}}_{i+1}^i + \beta (\Delta t)^2 \hat{\mathbf{K}}_{i+1}^i, \tag{19}$$

$$\mathbf{b}_{i+1}^i(t) = \bar{\mathbf{b}}_{i+1}^i(t) - \hat{\mathbf{q}}_{i+1}^i(t) + \hat{\mathbf{C}}_{i+1}^i \mathbf{h}_{i+1}^i(t) + \hat{\mathbf{K}}_{i+1}^i \mathbf{g}_{i+1}^i(t), \tag{20}$$

and Eqs. (19) and (20) are the point transfer rules of the mass coefficient matrix and the force corrective vector, respectively.

As shown in Fig. 3, we define the positive directions of the displacements $(u_x, u_y, u_z)_{i+1}^i$, the angular displacements $(\phi_x, \phi_y, \phi_z)_{i+1}^i$, the forces $(F_x, F_y, F_z)_{i+1}^i$ and the moments $(M_x, M_y, M_z)_{i+1}^i$ represented by the local coordinate system (X_{i+1}^i, Y_{i+1}^i, Z_{i+1}^i) fixed on the *i*–th beam element at the right-hand side of the (*i*+1)-th node. The positive directions of the dis-

placements $(u_x, u_y, u_z)_{i+1}^{i+1}$, the angular displacements $(\phi_x, \phi_y, \phi_z)_{i+1}^{i+1}$, the forces $(F_x, F_y, F_z)_{i+1}^{i+1}$ and the moments $(M_x, M_y, M_z)_{i+1}^{i+1}$ represented by the local coordinate system (X_{i+1}^{i+1}, Y_{i+1}^{i+1}, Z_{i+1}^{i+1}) fixed on the (*i*+1)-th beam element are illustrated in Fig. 3.

If the local coordinate system of the (*i*+1)-th beam element is rotated by the Euler angle, $\boldsymbol{\theta}_{i+1} = (\theta_1, \theta_2, \theta_3)_{i+1}$, from the local coordinate system of the *i*-th beam element, as shown in Fig. 4 [13], we obtain

$$\mathbf{a}_{i+1}^{i+1}(t) = \mathbf{T}(\boldsymbol{\theta}_{i+1})\mathbf{a}_{i+1}^{i}(t), \quad \mathbf{f}_{i+1}^{i+1}(t) = \mathbf{T}(\boldsymbol{\theta}_{i+1})\mathbf{f}_{i+1}^{i}(t), \quad (21)$$

where

$$\mathbf{T}(\boldsymbol{\theta}_{i+1}) = \begin{bmatrix} t_{11} & t_{12} & t_{13} & 0 & 0 & 0 \\ t_{21} & t_{22} & t_{23} & 0 & 0 & 0 \\ t_{31} & t_{32} & t_{33} & 0 & 0 & 0 \\ 0 & 0 & 0 & t_{11} & t_{12} & t_{13} \\ 0 & 0 & 0 & t_{21} & t_{22} & t_{23} \\ 0 & 0 & 0 & t_{31} & t_{32} & t_{33} \end{bmatrix}_{i+1},$$

$$\begin{aligned} t_{11} &= \cos\theta_2, \quad t_{12} = \cos\theta_1 \sin\theta_2, \\ t_{13} &= \sin\theta_1 \sin\theta_2, \quad t_{21} = -\sin\theta_2 \cos\theta_3, \\ t_{22} &= \cos\theta_1 \cos\theta_2 \cos\theta_3 - \sin\theta_1 \sin\theta_3, \\ t_{23} &= \sin\theta_1 \cos\theta_2 \cos\theta_3 + \cos\theta_1 \sin\theta_3, \\ t_{31} &= \sin\theta_2 \sin\theta_3, \\ t_{32} &= -\cos\theta_1 \cos\theta_2 \sin\theta_3 - \sin\theta_1 \cos\theta_3, \\ t_{33} &= -\sin\theta_1 \cos\theta_2 \sin\theta_3 + \cos\theta_1 \cos\theta_3, \end{aligned} \quad (22)$$

and the matrix $\mathbf{T}(\boldsymbol{\theta}_{i+1})$ has the following property:

$$\mathbf{T}(\boldsymbol{\theta}_{i+1})^{-1} = \mathbf{T}(\boldsymbol{\theta}_{i+1})^{\mathrm{T}}. \quad (23)$$

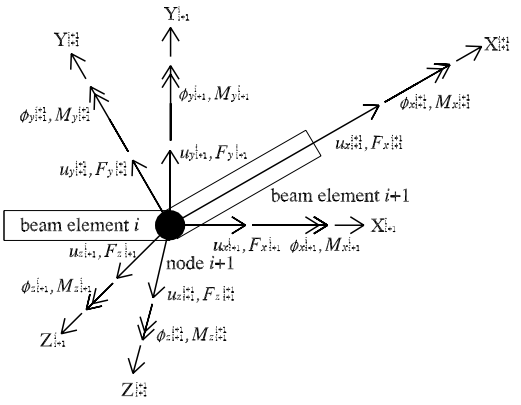

Fig. 3. Definition of positive direction of displacements and forces of crooked part.

We can obtain the matrix $\mathbf{J}_{i+1}^{i+1}$ and the vector $\mathbf{b}_{i+1}^{i+1}(t)$ represented by the local coordinate system of the (*i*+1)-th beam element from Eqs. (3), (4) and (21) as follows:

$$\mathbf{J}_{i+1}^{i+1} = \mathbf{T}(\boldsymbol{\theta}_{i+1})\mathbf{J}_{i+1}^{i}\mathbf{T}(\boldsymbol{\theta}_{i+1})^{\mathrm{T}}, \quad (24)$$

$$\mathbf{b}_{i+1}^{i+1}(t) = \mathbf{T}(\boldsymbol{\theta}_{i+1})\mathbf{b}_{i+1}^{i}(t), \quad (25)$$

Eqs. (24) and (25) are the coordinate transformation rules of the mass coefficient matrix and the force corrective vector, respectively.

If there are an additional mass, springs, viscous dampers and external forces at the first node, the balancing of the force at the first node yields

$$\hat{\mathbf{M}}_1^1\mathbf{a}_1^1(t) = \mathbf{f}_1^1(t) - \bar{\mathbf{f}}_1^1(t) - \hat{\mathbf{C}}_1^1\mathbf{v}_1^1(t) - \hat{\mathbf{K}}_1^1\mathbf{d}_1^1(t) + \hat{\mathbf{q}}_1^1(t). \quad (26)$$

Because the left-hand boundary condition of the structure is modeled as the point stiffness matrix ($\hat{\mathbf{K}}_1^1$) and damping matrix ($\hat{\mathbf{C}}_1^1$) at the first node in the present method, the force vector $\bar{\mathbf{f}}_1^1(t)$ can be considered as a null vector. Therefore, we can find the matrix $\mathbf{J}_1^1$ and the vector $\mathbf{b}_1^1(t)$ from $\bar{\mathbf{f}}_1^1(t) = \mathbf{0}$, Eq. (26) and the equations obtained by substituting 1 into *i* in Eqs. (1) and (6) as follows:

$$\mathbf{J}_1^1 = \hat{\mathbf{M}}_1^1 + \gamma\Delta t\hat{\mathbf{C}}_1^1 + \beta(\Delta t)^2\hat{\mathbf{K}}_1^1, \quad (27)$$

$$\mathbf{b}_1^1(t) = \hat{\mathbf{C}}_1^1\mathbf{h}_1^1(t) + \hat{\mathbf{K}}_1^1\mathbf{g}_1^1(t) - \hat{\mathbf{q}}_1^1(t). \quad (28)$$

After finding the matrix $\mathbf{J}_1^1$ from Eq. (27), we successively apply Eqs. (14), (19) and (24) for the analytical model. Therefore, we can obtain the matrix $\mathbf{J}_{n+1}^{n}$ at the right-hand side of the (*n*+1)-th node, that is, the last node. In the same manner, after obtaining the vector $\mathbf{b}_1^1(t)$ from Eq. (28), we successively

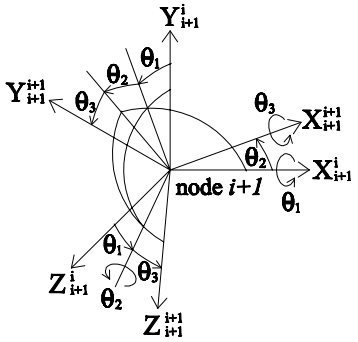

Fig. 4. Definition of the Euler angle.

apply Eqs. (15), (20) and (25). Finally, we can obtain the vector $\mathbf{b}^{n}_{n+1}(t)$.

2.3 Dynamic response

Because the right-hand boundary condition of the structure is modeled as the point stiffness matrix ($\hat{\mathbf{K}}^{n}_{n+1}$) and damping matrix ($\hat{\mathbf{C}}^{n}_{n+1}$) at the ($n$+1)-th node in the present method, the force vector $\mathbf{f}^{n}_{n+1}(t)$ can be considered as a null vector. From $\mathbf{f}^{n}_{n+1}(t)=\mathbf{0}$ and the equation obtained by substituting (n+1) into i in Eq. (3), the acceleration vector of the (n+1)-th node can be obtained as follows:

$$\mathbf{a}^{n}_{n+1}(t) = -(\mathbf{J}^{n}_{n+1})^{-1}\,\mathbf{b}^{n}_{n+1}(t). \tag{29}$$

From Eqs. (1), (2), (5), (12) and (16), the relationship of the acceleration vectors between the left- and right-hand sides of the the i-th beam element is given as

$$\mathbf{a}^{i}_{i}(t) = \mathbf{B}^{i}_{i}\,\mathbf{a}^{i}_{i+1}(t) + \mathbf{w}^{i}_{i}(t)\ . \tag{30}$$

From the equations obtained by substituting i-1 into i in Eqs. (21) and (23), the following equation can be obtained:

$$\mathbf{a}^{i-1}_{i}(t) = \mathbf{T}(\boldsymbol{\theta}_{i})^{\mathrm{T}}\,\mathbf{a}^{i}_{i}(t)\ . \tag{31}$$

After the acceleration vector of the (n+1)-th node is calculated from Eq. (29), the acceleration vectors at the other nodes can be obtained recursively by using Eqs. (30) and (31). Therefore, the displacement and velocity vectors of all nodes at the time t can be derived from Eqs. (6) and (7) after the acceleration vectors at the time t are calculated.

2.4 Initial acceleration

At the initial time, t=0, Eq. (11) becomes:

$$\mathbf{M}^{i}_{i}\begin{Bmatrix}\mathbf{a}^{i}_{i}(0)\\ \bar{\mathbf{a}}^{i}_{i+1}(0)\end{Bmatrix}+\mathbf{C}^{i}_{i}\begin{Bmatrix}\mathbf{v}^{i}_{i}(0)\\ \bar{\mathbf{v}}^{i}_{i+1}(0)\end{Bmatrix}+\mathbf{K}^{i}_{i}\begin{Bmatrix}\mathbf{d}^{i}_{i}(0)\\ \bar{\mathbf{d}}^{i}_{i+1}(0)\end{Bmatrix}=\begin{Bmatrix}-\mathbf{f}^{i}_{i}(0)\\ \bar{\mathbf{f}}^{i}_{i+1}(0)\end{Bmatrix}. \tag{32}$$

From Eq. (32), the following equation can be obtained.

$$\begin{bmatrix}\tilde{\mathbf{P}}^{i}_{i} & \tilde{\mathbf{Q}}^{i}_{i}\\ \tilde{\mathbf{R}}^{i}_{i} & \tilde{\mathbf{S}}^{i}_{i}\end{bmatrix}\begin{Bmatrix}\mathbf{a}^{i}_{i}(0)\\ \bar{\mathbf{a}}^{i}_{i+1}(0)\end{Bmatrix}+\begin{Bmatrix}\tilde{\mathbf{y}}^{i}_{i}(0)\\ \tilde{\mathbf{y}}^{i}_{i+1}(0)\end{Bmatrix}=\begin{Bmatrix}-\mathbf{f}^{i}_{i}(0)\\ \bar{\mathbf{f}}^{i}_{i+1}(0)\end{Bmatrix}, \tag{33}$$

where

$$\begin{bmatrix}\tilde{\mathbf{P}}^{i}_{i} & \tilde{\mathbf{Q}}^{i}_{i}\\ \tilde{\mathbf{R}}^{i}_{i} & \tilde{\mathbf{S}}^{i}_{i}\end{bmatrix}=\mathbf{M}^{i}_{i},\qquad \begin{Bmatrix}\tilde{\mathbf{y}}^{i}_{i}(0)\\ \tilde{\mathbf{y}}^{i}_{i+1}(0)\end{Bmatrix}=\mathbf{C}^{i}_{i}\begin{Bmatrix}\mathbf{v}^{i}_{i}(0)\\ \bar{\mathbf{v}}^{i}_{i+1}(0)\end{Bmatrix}+\mathbf{K}^{i}_{i}\begin{Bmatrix}\mathbf{d}^{i}_{i}(0)\\ \bar{\mathbf{d}}^{i}_{i+1}(0)\end{Bmatrix}. \tag{34}$$

The field transfer rules of the mass coefficient matrix and the force corrective vector at the initial time can be obtained from Eqs. (1) and (2) at t=0 and Eq. (33) as follows:

$$\bar{\mathbf{J}}^{i}_{i+1} = \tilde{\mathbf{R}}^{i}_{i}\tilde{\mathbf{B}}^{i}_{i} + \tilde{\mathbf{S}}^{i}_{i}, \tag{35}$$

$$\bar{\mathbf{b}}^{i}_{i+1}(0) = \tilde{\mathbf{R}}^{i}_{i}\tilde{\mathbf{w}}^{i}_{i}(0) + \tilde{\mathbf{y}}^{i}_{i+1}(0), \tag{36}$$

where

$$\tilde{\mathbf{B}}^{i}_{i} = \tilde{\mathbf{A}}^{i}_{i}\tilde{\mathbf{Q}}^{i}_{i},\quad \tilde{\mathbf{w}}^{i}_{i}(0) = \tilde{\mathbf{A}}^{i}_{i}\left\{\mathbf{b}^{i}_{i}(0) + \tilde{\mathbf{y}}^{i}_{i}(0)\right\},\qquad \tilde{\mathbf{A}}^{i}_{i} = -(\tilde{\mathbf{P}}^{i}_{i} + \mathbf{J}^{i}_{i})^{-1}. \tag{37}$$

From the balancing of the forces and the moments of the (i+1)-th node at the initial time, we obtain

$$\hat{\mathbf{M}}^{i}_{i+1}\mathbf{a}^{i}_{i+1}(0) = \mathbf{f}^{i}_{i+1}(0) - \bar{\mathbf{f}}^{i}_{i+1}(0) - \hat{\mathbf{C}}^{i}_{i+1}\mathbf{v}^{i}_{i+1}(0) - \hat{\mathbf{K}}^{i}_{i+1}\mathbf{d}^{i}_{i+1}(0) + \hat{\mathbf{q}}^{i}_{i+1}(0). \tag{38}$$

The point transfer rules of the mass coefficient matrix and the force corrective vector at the initial time can be obtained from Eqs. (2), (3) and (5) at t=0 and Eq. (38) as follows:

$$\mathbf{J}^{i}_{i+1} = \bar{\mathbf{J}}^{i}_{i+1} + \hat{\mathbf{M}}^{i}_{i+1}, \tag{39}$$

$$\mathbf{b}^{i}_{i+1}(0) = \bar{\mathbf{b}}^{i}_{i+1}(0) - \hat{\mathbf{q}}^{i}_{i+1}(0) + \hat{\mathbf{C}}^{i}_{i+1}\mathbf{v}^{i}_{i+1}(0) + \hat{\mathbf{K}}^{i}_{i+1}\mathbf{d}^{i}_{i+1}(0). \tag{40}$$

From the balancing of the forces and the moments of the first node at the initial time, we obtain

$$\hat{\mathbf{M}}^{1}_{1}\mathbf{a}^{1}_{1}(0) = \mathbf{f}^{1}_{1}(0) - \bar{\mathbf{f}}^{1}_{1}(0) - \hat{\mathbf{C}}^{1}_{1}\mathbf{v}^{1}_{1}(0) - \hat{\mathbf{K}}^{1}_{1}\mathbf{d}^{1}_{1}(0) + \hat{\mathbf{q}}^{1}_{1}(0). \tag{41}$$

At the initial time, the mass coefficient matrix $\mathbf{J}^{1}_{1}$ and the force corrective vector $\mathbf{b}^{1}_{1}(0)$ of the first node can be obtained from $\bar{\mathbf{f}}^{1}_{1}(0)=\mathbf{0}$, Eq. (1) at t=0 and Eq. (41) as follows:

$$\mathbf{J}_1^1 = \hat{\mathbf{M}}_1^1, \tag{42}$$

$$\mathbf{b}_1^1(0) = \hat{\mathbf{C}}_1^1 \mathbf{v}_1^1(0) + \hat{\mathbf{K}}_1^1 \mathbf{d}_1^1(0) - \hat{\mathbf{q}}_1^1(0). \tag{43}$$

After finding the matrix $\mathbf{J}_1^1$ from Eq. (42), we successively apply Eqs. (35) and (39), and Eq. (24) at t=0 for analytical model. Therefore, we can obtain the matrix $\mathbf{J}_{n+1}^n$. In the same manner, after obtaining the vector $\mathbf{b}_1^1(0)$ from Eq. (43), we successively apply Eqs. (36) and (40), and Eq. (25) at t=0. Finally, we can obtain the vector $\mathbf{b}_{n+1}^n(0)$.

From Eqs. (1), (2) and (5) at t=0, and Eqs. (33) and (37), the relationship of the acceleration vectors between the left- and right-hand sides of the i-th beam element is given as

$$\mathbf{a}_i^i(0) = \tilde{\mathbf{B}}_i^i \mathbf{a}_{i+1}^i(0) + \bar{\mathbf{w}}_i^i(0) \ . \tag{44}$$

The initial acceleration vector of the (n+1)-th node can be obtained from Eq. (29) at t=0. The initial acceleration vectors at the other nodes can be obtained recursively by using Eqs. (44) and Eq. (31) at t=0.

3. Numerical examples

We made two computer programs based on the TMCM and DIM. In this paper, the plane and space beam structures are chosen as the numerical models. The response results and computation times of the TMCM are compared with those of the DIM under the same condition to verify the computational accuracy and efficiency of the TMCM.

3.1 Example 1

The first numerical model is a linearly tapered cantilever beam of solid rectangular cross-section, as shown in Fig. 5. The physical parameters of the beam are as follows: mass density 7860 kg/m^3, Young's modulus 206 GPa. The beam has a viscous damper (c_y= 100 Ns/m) at the right-hand end; the structural damping of the beam is neglected. The beam is initially at rest and is subjected to a step load (q_y= 2000 N) at the right-hand end. Each node of the beam has two degrees-of-freedom in the first numerical model.

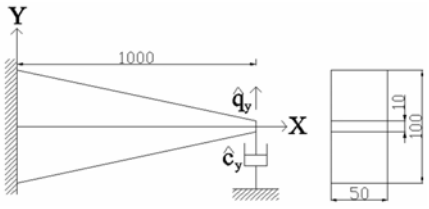

Fig. 5. Linearly tapered cantilever beam.

In numerical calculation, the linearly tapered beam is simply modeled as a large number of beam elements. Each element has constant rectangular cross-section whose area linearly decreases from the first

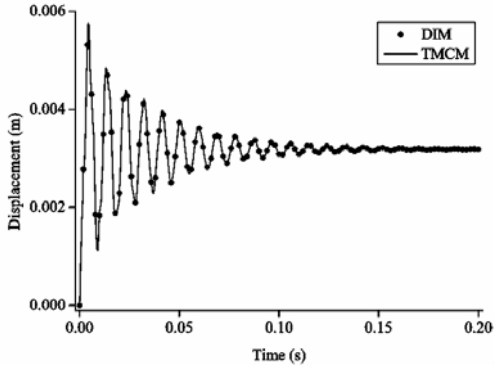

Fig. 6. Dynamic response of linearly tapered cantilever beam subjected to step load.

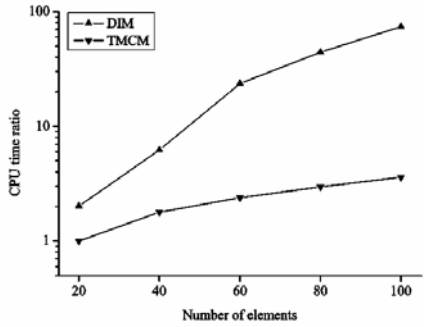

Fig. 7. Comparison of computation times for linearly tapered cantilever beam.

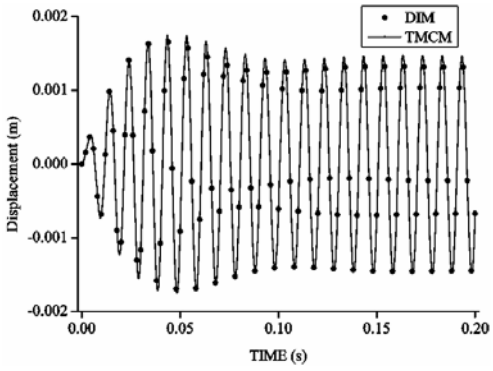

Fig. 8. Dynamic response of linearly tapered cantilever beam subjected to periodic load.

beam element to the last beam element. The mass of the beam is considered as the consistent mass modeling. Because the boundary condition of the beam is fixed-free, the numerical model has two springs supporting the first node. The values of the spring constants of the first node are considered as 1.0E20. The time step is 0.0001 s, and the total response time is 0.2 s. The parameters β and γ of Newmark's β method are considered as 0.25 and 0.5, respectively.

After the beam is divided into 20, 40, 60, 80 and 100 beam elements, the results computing the dynamic responses of the right-hand end of the beam by the TMCM coincide completely with those by the DIM. Fig. 6 shows the displacement (u_y) of the right-hand end of the beam modeled as the 100 beam elements, calculated by the TMCM and DIM. To distinctly show the response results of both methods in Fig. 6, the result of the TMCM is represented by the solid line, that of the DIM is represented as only 101 symbols, because the number of time points of the dynamic response is very large and both results coincide with each other. The results of the DIM in Fig. 8, Fig. 10 and Fig. 11 are represented as only 101 symbols, for the same reason as Fig. 6.

Fig. 7 shows computation time ratio by both methods according to the number of the beam elements, where the computation time used for obtaining dynamic response of the beam modeled as 20 beam elements by the TMCM is defined as one. It is found from Fig. 7 that the TMCM is superior to the DIM in respect to computation time. In particular, the difference of computation times by both methods largely increases according to the number of the used beam elements.

When the above beam is subjected to in-plane periodic load at the right-hand end ($\hat{q}_y$ =A sin ωt, A=200 N, ω=100 Hz), Fig. 8 shows the displacement (u_y) of the right-hand end of the beam modeled as 100 beam elements, obtained by the TMCM and the DIM. The results obtained by the TMCM agree well with those by the DIM, too.

If the beam is modeled as 100 beam elements, the total degrees-of-freedom of the numerical model is 202. Then, in the DIM, the sizes of the total mass, damping and stiffness matrices are 202 by 202. However, the size of the mass coefficient matrix in the TMCM is only 2 by 2. Therefore, the TMCM is superior to the DIM in respect to computation memory, because the TMCM uses the small size of matrix through the transfer rules.

3.2 Example 2

The second numerical model is a three-dimensional beam structure with many crooked parts and supports. The total length of the structure is 6.8 m. The physical parameters of the beam are as follows: mass density 7860 kg/m^3, Young's modulus 206 GPa, shear modulus 79.2 GPa.

In numerical calculation, the structure is modeled as 34, 68, 102, 136 and 170 straight-line beam elements with the circular cross-section of diameter 5 cm. Fig. 9 shows the numerical model having 34 beam elements. For the structure modeled as 34 beam elements, the length of all beam elements is equally 0.2 m, and the structure has springs and viscous dampers at nodes 1, 2, 10, 18, 26, and 34. All constants of springs and viscous dampers are as follows:

$$\hat{k}_{x1}^{\ 1} = \hat{k}_{y2}^{\ 1} = \hat{k}_{z2}^{\ 1} = \hat{k}_{y10}^{\ 9} = \hat{k}_{z10}^{\ 9} = \hat{k}_{y18}^{\ 17} = \hat{k}_{z18}^{\ 17} =$$
$$\hat{k}_{y26}^{\ 25} = \hat{k}_{z26}^{\ 25} = \hat{k}_{y34}^{\ 33} = \hat{k}_{z34}^{\ 33} = 10^5 \text{ N/m},$$
$$\hat{c}_{1x}^{\ 1} = \hat{c}_{2y}^{\ 1} = \hat{c}_{2z}^{\ 1} = \hat{c}_{y10}^{\ 9} = \hat{c}_{z10}^{\ 9} = \hat{c}_{y18}^{\ 17} = \hat{c}_{z18}^{\ 17} =$$
$$\hat{c}_{y26}^{\ 25} = \hat{c}_{z26}^{\ 25} = \hat{c}_{y34}^{\ 33} = \hat{c}_{z34}^{\ 33} = 200 \text{ Ns/m}.$$

The mass of the beam is considered as the consistent mass modeling. The structural damping is neglected. The time step is 0.001 s, and the total response time is 3 s. The parameters β and γ of Newmark's β method are considered as 0.25 and 0.5, respectively.

The structure is initially at rest and is subjected to periodic load ($\hat{q}_y$ =A sin ωt, A=2000 N, ω=1 Hz) at the location of node 6 for the structure modeled as 34 beam elements. Each node of the structure has six

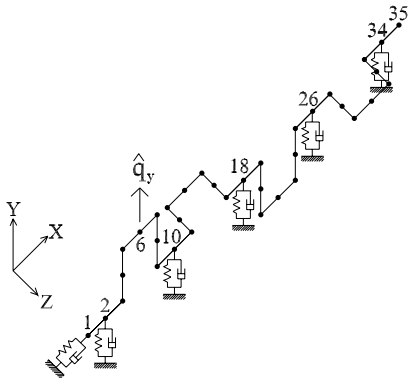

Fig. 9. Three-dimensional beam structure modeled as 34 beam elements.

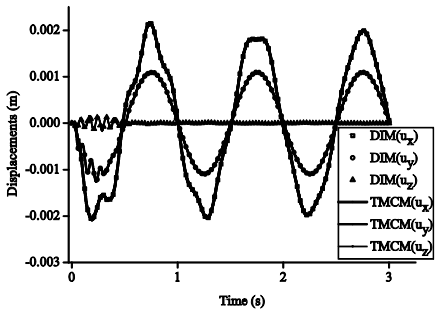

Fig. 10. Dynamic response of the right-hand end of three-dimensional beam structure.

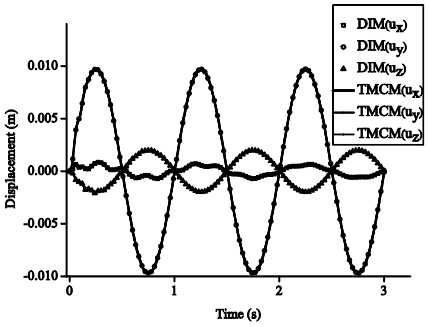

Fig. 11. Dynamic response of excitation point of three-dimensional beam structure.

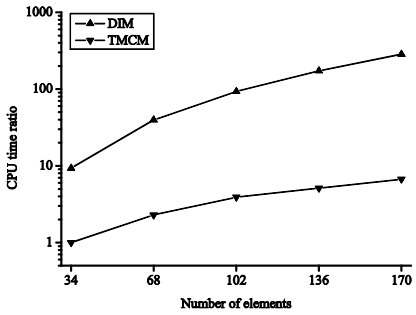

Fig. 12. Comparison of computation times for three-dimensional beam structure.

degrees-of-freedom in the second numerical model.

After the structure is divided into 34, 68, 102, 136 and 170 beam elements, respectively, the results computing the dynamic responses of the structure by the TMCM coincide completely with those by the DIM. Fig. 10 shows the displacements (u_x, u_y, u_z) of the right-hand end of the structure modeled as 170 beam elements, obtained by the TMCM and the DIM. Fig. 11 shows the displacements of the excitation point of the structure modeled as 170 beam elements, obtained by both methods.

Fig. 12 shows computation time ratio by both methods according to the number of the used beam elements, where the computation time used for obtaining dynamic response of the structure modeled as 34 beam elements by the TMCM is defined as one. It is found from Fig. 12 that the TMCM is superior to the DIM in respect to computation time, too.

For the beam modeled as 170 beam elements, the total degrees-of-freedom of system is 1026. Then, in the DIM, the sizes of the total mass, damping and stiffness matrices are 1026 by 1026. However, the size of the mass coefficient matrix in the TMCM is only 6 by 6.

When we obtain the dynamic response of a beam structure by the DIM, the sizes of the mass, damping and stiffness matrices are equal to the total number of degrees-of-freedom for the beam structure. Therefore, large computer memory and long computation time are required to analyze the beam structure with very large degrees-of-freedom by the DIM. However, the TMCM can greatly reduce computation time in spite of using small computer memory by using the transfer rules successively.

4. Conclusions

We developed the transfer mass coefficient method for effectively computing the dynamic response of various beam structures modeled as lumped mass, consistent mass, viscous damper, structural damping and Rayleigh-type damping. The concept of the present method is based on both the transfer technique of the mass coefficient and the numerical integration technique such as Newmark's β method.

In this paper, the algorithm for the dynamic response analysis of a three-dimensional beam structure is formulated by the transfer mass coefficient method. Plane and space beam structures are chosen as numerical models. The response results and computation times obtained by the transfer mass coefficient method were compared with those obtained by the direct integration method under the same condition. We verified that the transfer mass coefficient method can remarkably decrease the computation time of the direct integration method without the loss of accuracy in spite of using small computer memory.

Acknowledgment

This work was supported by the Innovation 06

funded by the Fisheries Research Institute of Chonnam National University.

References

[1] J. W. Tedesco, W. G. McDougal and C. A. Ross, *Structural dynamics theory and applications*, Addison Wesley Longman, California, USA, (1999).

[2] K. J. Bathe, *Finite element procedures*, Prentice-Hall, New Jersey, USA, (1996).

[3] M. Petyt, *Introduction to finite element vibration analysis*, Cambridge University Press, Cambridge, England, (1990).

[4] H. Yamakawa and T. Ohnishi, Dynamic response analysis of structures with large degrees of freedom by step-by-step transfer matrix method, *Bulletin of the JSME*, 26 (211) (1983) 109-116.

[5] A. S. Kumar and T. S. Sankar, A new transfer matrix method for response analysis of large dynamic systems, *Computers & Structures*, 23 (4) (1986) 545-552.

[6] M. Ohga and T. Shigematsu, Transient analysis of plates by a combined finite element-transfer matrix method, *Computers & Structures*, 26 (4) (1987) 543-549.

[7] M. Ohga, T. Shigematsu and T. Hara, A finite element-transfer matrix method for dynamic analysis of frame structures, *J. Sound and Vibration*, 167 (3) (1993) 401-411.

[8] H. Xue, A combined finite element-riccati transfer matrix method in frequency domain for transient structural response, *Computers & Structures*, 62 (2) (1997) 215-220.

[9] A. S. Ashour and A. M. Farag, A combination between Laplace transform, strip method and transition matrix for determination of dynamic response and damping effect of plates, *International Journal of Acoustics and Vibration*, 5 (4) (2000) 191-195.

[10] T. Inoue, A. Sueoka and T. Fusimoto, Time historical response analysis of large-scaled structures (improvement of computational efficiency and numerical stability by applying the transfer influence coefficient method), *Trans. of JSME*, Series C, 62 (604) (1996) 4558-4566.

[11] E. C. Pestel and F. A. Leckie, *Matrix methods in elastomechanics*, McGraw-Hill, New York, USA, (1963).

[12] A. Sueoka, T. Koudou, D. H. Moon, K. Yamashita and H. Tamura, Free vibration analysis of a multiple straight line structure regarded as a discrete system by the transfer influence coefficient method, *JSME International Journal*, Series Ⅲ, 32 (1) (1989) 10-18.

[13] T. Koudou, A. Sueoka, Y. Yasuda and D. H. Moon, Free vibration analysis of a tree structure by the transfer influence coefficient method (2nd report, treatment of a three-dimensional tree structure and numerical computational results), JSME International Journal, Series Ⅲ, 35 (1) (1992) 32-40.

[14] L. L. Logan, *A first course in the finite element method*, PWS Publishing Company, Boston, USA, (1993).

[15] Y. W. Kwon and H. Bang, *The finite element method using Matlab*, Second Ed., CRC Press, New York, USA, (2000) 237-306.

[16] S. G. Kelly, *Fundamentals of mechanical vibrations*, Second Ed., McGraw-Hill, International Editions, (2000) 501-534.

Appendix

Mass, stiffness and damping matrices of beam element [3, 15, 16]

The mass matrix of the i-th beam element representing by the local coordinate system fixed on the i-th beam element is

$$\mathbf{M}_{\mathbf{i}}^{\mathbf{i}} = \begin{bmatrix} \mathbf{M}_{11} & \mathbf{M}_{12} \\ \mathbf{M}_{12}^{\mathbf{T}} & \mathbf{M}_{22} \end{bmatrix}_{\mathbf{i}}^{\mathbf{i}}, \tag{A.1}$$

where

$$\mathbf{M}_{11} = \begin{bmatrix} m_1 & 0 & 0 & 0 & 0 & 0 \\ 0 & m_2 & 0 & 0 & 0 & m_5 \\ 0 & 0 & m_2 & 0 & -m_5 & 0 \\ 0 & 0 & 0 & m_3 & 0 & 0 \\ 0 & 0 & -m_5 & 0 & m_4 & 0 \\ 0 & m_5 & 0 & 0 & 0 & m_4 \end{bmatrix}, \tag{A.2}$$

$$\mathbf{M}_{12} = \begin{bmatrix} m_6 & 0 & 0 & 0 & 0 & 0 \\ 0 & m_7 & 0 & 0 & 0 & m_{10} \\ 0 & 0 & m_7 & 0 & -m_{10} & 0 \\ 0 & 0 & 0 & m_8 & 0 & 0 \\ 0 & 0 & m_{10} & 0 & m_9 & 0 \\ 0 & -m_{10} & 0 & 0 & 0 & m_9 \end{bmatrix}, \tag{A.3}$$

$$\mathbf{M}_{22}=\begin{bmatrix} m_1 & 0 & 0 & 0 & 0 & 0 \\ 0 & m_2 & 0 & 0 & 0 & -m_5 \\ 0 & 0 & m_2 & 0 & m_5 & 0 \\ 0 & 0 & 0 & m_3 & 0 & 0 \\ 0 & 0 & m_5 & 0 & m_4 & 0 \\ 0 & -m_5 & 0 & 0 & 0 & m_4 \end{bmatrix}. \quad \text{(A.4)}$$

In which $m_1=\rho AL/3$, $m_2=13\rho AL/35$, $m_3=\rho LI_X/3$, $m_4=\rho AL^3/105$, $m_5=11\rho AL^2/210$, $m_6=\rho AL/6$, $m_7=9\rho AL/70$, $m_8=\rho LI_X/6$, $m_9=-\rho AL^3/140$ and $m_{10}=-13\rho AL^2/420$ where L, ρ, A and I_X are the length of the beam, the mass density, the cross-sectional area and the second moment of area of the cross-section about the X-axis, respectively.

The stiffness matrix of the *i*-th beam element representing by the local coordinate system fixed on the *i*-th beam element is

$$\mathbf{K}_{\mathbf{i}}^{\mathbf{i}}=\begin{bmatrix} \mathbf{K}_{11} & \mathbf{K}_{12} \\ \mathbf{K}_{12}^{\mathbf{T}} & \mathbf{K}_{22} \end{bmatrix}_{\mathbf{i}}^{\mathbf{i}}, \quad \text{(A.5)}$$

where

$$\mathbf{K}_{11}=\begin{bmatrix} k_1 & 0 & 0 & 0 & 0 & 0 \\ 0 & k_2 & 0 & 0 & 0 & k_8 \\ 0 & 0 & k_3 & 0 & k_7 & 0 \\ 0 & 0 & 0 & k_4 & 0 & 0 \\ 0 & 0 & k_7 & 0 & k_5 & 0 \\ 0 & k_8 & 0 & 0 & 0 & k_6 \end{bmatrix}, \quad \text{(A.6)}$$

$$\mathbf{K}_{12}=\begin{bmatrix} -k_1 & 0 & 0 & 0 & 0 & 0 \\ 0 & -k_2 & 0 & 0 & 0 & k_8 \\ 0 & 0 & -k_3 & 0 & k_7 & 0 \\ 0 & 0 & 0 & -k_4 & 0 & 0 \\ 0 & 0 & -k_7 & 0 & k_9 & 0 \\ 0 & -k_8 & 0 & 0 & 0 & k_{10} \end{bmatrix}, \quad \text{(A.7)}$$

$$\mathbf{K}_{22}=\begin{bmatrix} k_1 & 0 & 0 & 0 & 0 & 0 \\ 0 & k_2 & 0 & 0 & 0 & -k_8 \\ 0 & 0 & k_3 & 0 & -k_7 & 0 \\ 0 & 0 & 0 & k_4 & 0 & 0 \\ 0 & 0 & -k_7 & 0 & k_5 & 0 \\ 0 & -k_8 & 0 & 0 & 0 & k_6 \end{bmatrix}. \quad \text{(A.8)}$$

In which $k_1=EA/L$, $k_2=12EI_Z/L^3$, $k_3=12EI_Y/L^3$, $k_4=GJ/L$, $k_5=4EI_Y/L$, $k_6=4EI_Z/L$, $k_7=-6EI_Y/L^2$, $k_8=6EI_Z/L^2$, $k_9=2EI_Y/L$ and $k_{10}=2EI_Z/L$, where E, G, J, I_Y and I_Z are the Young's modulus of the material, the shear modulus, the torsion constant of the cross-section, the second moments of area of the cross-section about the Y-axis and Z-axis.

The damping matrix for the *i*-th beam element can be considered as a linear combination of the mass and stiffness matrix as follows:

$$\mathbf{C}_{\mathbf{i}}^{\mathbf{i}}=a\mathbf{M}_{\mathbf{i}}^{\mathbf{i}}+b\mathbf{K}_{\mathbf{i}}^{\mathbf{i}}, \quad \text{(A.9)}$$

where a and b are constants.

Myung-Soo Choi received his B.S. and M.S. degrees from National Fisheries University of Pusan, Korea, in 1992 and 1994, respectively. He then received his Ph.D. degree from Pukyong National University in 1999. Dr. Choi is currently an Assistant Professor at the Department of Maritime Police Science at Chonnam National University in Yeosu, Korea. His research interests include mechanical vibration, structural dynamics, and optimum design.

Dong-Jun Yeo received his B.S., M.S. and Ph.D. degrees from National Fisheries University of Pusan, Korea, in 1981, 1985 and 1996, respectively. Dr. Yeo is currently a Professor at the Faculty of Marine Technology at Chonnam National University in Yeosu, Korea. He serves as an Academic Director of the Korean Society for Power System Engineering. His research interests include structural dynamics, vibration, and analytic techniques.

Jung-Hwan Byun received his B.S. and M.S. degrees from National Fisheries University of Pusan, Korea, in 1992 and 1995, respectively. He then received his Ph.D. degree from Pukyong National University in 1997. Dr. Byun is currently an Associate Professor at the Faculty of Marine Technology at Chonnam National University in Yeosu, Korea. His research interests include numerical analysis and synchronous control.

Jung-Joo Suh received his B.S., M.S. and Ph.D. degrees from National Fisheries Uni-versity of Pusan, Korea, in 1972, 1985 and 1995, respec-tively. Dr. Suh is currently a Professor at the Faculty of Marine Technology at Chonnam National University in Yeosu, Korea. His research interests include internal combustion engines and numerical analysis.

Jung-Kyu Yang received his B.S. degree from Pusan Fisherise College, Korea, in 1973. He then received his M.S. and Ph.D. degrees from Chungnam National University in 1985 and 1996, respectively. Dr. Yang is currently a Professor at the Faculty of Marine Technology at Chonnam University in Yeosu, Korea. His research interests include combustion engineering, air flow characteristics, and numerical analysis.